

Dynamics of interstitial molecular-type double donor complexes in silicon

S.G. Pavlov^{b,*}, N. Deßmann^a, N.V. Abrosimov^c

^a Institute of Space Research, German Aerospace Center (DLR), Berlin, Germany

^b Radboud University, Institute for Molecules and Materials, HFML-FELIX, Nijmegen, the Netherlands

^c Leibniz-Institut für Kristallzüchtung (IKZ), Berlin, Germany

ARTICLE INFO

Keywords:

Molecular Mg double donors
Silicon
Time-resolved spectroscopy

ABSTRACT

Complementary time-resolved spectroscopies have been applied to study dynamics of molecular-type magnesium-related donors. Large interstate energy gaps of these donors prevent nonradiative decays through a first-order, one-phonon-assisted scattering – the main relaxation mechanism in shallow substitutional donors in low-doped silicon. Analysis reveals very short decay times of the deepest excited states of molecular donors: dephasing within less than 10 ps and relaxation rates above 30 ns^{-1} . These decays are several times shorter than those observed in single-electron hydrogen-like substitutional donors, but longer than those in helium-like interstitial atomic magnesium centers in silicon. Spectral correlations of temporal dependences of particular transients to the lattice phonon overtones suggest that phonon-assisted electronic scattering contributes also to decoherence of states in these double donors. Such efficient second-order phonon-assisted processes were underestimated for dynamics of deep impurities in semiconductors.

1. Introduction

Molecular-type electrically-active impurity' complexes exhibit diverse properties, strongly dependent on the type of bound atoms. Such complexes have, in general, at least one defect (among others also vacancies V or host atoms not at the lattice site) or one interstitial center (X_i), which determines most of characteristic features in the molecular energy spectrum, lifetimes of occupied electronic states, coupling to other defects and to the host semiconductor lattice, long-term chemical stability.

Obviously, multi-atomic impurity complexes can extend and modify physical properties of classical semiconductors doped by single atoms, due to expanding complexity and often - versatility of electronic configurations [1].

The applicability of such modified material covers different areas of research and developments [2], offering ultra-precise, nanoscale detection of magnetic fields, electric fields, and temperature, such as nitrogen vacancy NV^- centers in diamond [3] but also pushing everyday photovoltaic industry or optoelectronics [4]. Molecular T-centers (C-C-H) are promising quantum defects for silicon-based quantum networks due to its telecommunications-band optical emission and long-lived, submicrosecond optical lifetimes and nuclear spin coherence (above 1 s) achieved at cryogenic temperature in isotopically enriched

^{28}Si [5].

To investigate the potential of molecular complexes for optoelectronic devices, key properties to explore include optical (absorption/spectral range), electronic (energy spectra of defects), structural and chemical properties (bond long-term stability, stiffness) and processability. Understanding charge carrier dynamics is crucial for optimizing performance, alongside factors like cost-effectiveness and fabrication scalability for commercial viability.

Magnesium (divalent) atoms in silicon have been found recently to be able to form a large number of optically active donors with various binding energies [6,7].

Such a broad spectrum of Mg-related molecular donors (we shall call them further Mg-X) covers the spectral range between hydrogen-like, shallow, substitutional (X_s) single-electron (group-V, pentavalent) donors and deeper, helium-like two-electron (group-VI, hexavalent) substitutional donor centers. This may open perspectives for optoelectronic devices operating between far- and mid-infrared spectral ranges, including the atmospheric window of 8–14 μm .

Dynamic properties of molecular-type donors formed in silicon lattice are also of an excessive interest due to the opportunity to study coherence of these centers upon external excitation. Direct comparison between atomic and molecular donors embedded into a solid lattice is of special interest when compared with their analogs in gaseous matter,

* Corresponding author.

E-mail address: sergeij.pavlov@dlr.de (S.G. Pavlov).

<https://doi.org/10.1016/j.mssp.2025.110158>

Received 24 June 2025; Received in revised form 1 October 2025; Accepted 15 October 2025

Available online 23 October 2025

1369-8001/© 2025 The Authors. Published by Elsevier Ltd. This is an open access article under the CC BY license (<http://creativecommons.org/licenses/by/4.0/>).

where the coherence time scales for such type of species are very different [8]. Molecular energy spectra increase their complexity with the number of atoms and intermolecular bonds; at the same time coherence of electronic states and lifetimes of vibrational excitations decrease [9].

Both intermolecular bonds and also coupling of impurity atoms to atoms of a host lattice can affect dynamics/coherence of such centers.

Dynamic properties of substitutional centers in a low-doped semiconductor lattice at low temperatures have been shown to be governed by interaction of electrons bound to donor states and a single lattice vibrational mode (phonon), both theoretically and experimentally, see for instance the Review [10]. Molecular complexes can exhibit additional properties caused by vibrational modes inside the molecule. These are between an impurity atom and a lattice atom as well as those inherent for their host atom if different from the lattice one (i.e. defect) or a vacancy. Interstitial Mg atoms presume to form novel vibrational properties due to its different ways to bond to Si atoms.

This study aims to determine the characteristic lifetimes of molecular double Mg-X centers in silicon as well as obtaining insights in processes determining/contributing to the state' decay. Time-resolved single-frequency techniques, such as pump-probe, transient grating and photon echo, are widely used to study electronic dynamics. Being valuable analytical methods, they compromise the accuracy of complex electronic systems with multi-level energy spectra. As we recently demonstrated [11], combining several proper techniques significantly improves the accuracy of the results and helps avoid misinterpretation of observed transients. We used the mentioned above complementary time-resolved spectroscopies to derive decay times of excited electronic states. Analysis of the evolution of transient intensities puts energy-dependent constraints on dynamics of donor states. These dependences can link donor-phonon resonances and by this – to judge a strength of lattice-phonon-assisted scattering in the total decay rate of a particular state.

Impurity-lattice interactions can be predicted and evaluated on the

basis of the impurity energy spectra and the lattice phonon properties.

2. Magnesium molecular-type double donors

2.1. State-of-the-art knowledge on structure and dynamics

At present, information on the dynamics of molecular double Mg-related donors in silicon is limited to those obtained indirectly, by marking the characteristic time ranges that could match to the limits obtained in their frequency-domain spectra: from the linewidths of the corresponding absorption lines of the donor intracenter transitions.

The energy spectra of double donors in silicon resemble many properties of a helium atom.

While the Rydberg-like excited states of Mg-related donors almost replicate those of substitutional, single-atom donor centers [12], chemical shifts of their ground states and its valley-orbit-split (VOS) states (Fig. 1) appear to be dependent on the type of bonding of interstitial atoms to lattice atoms and, apparently, on a center symmetry, if the latter differs from a conventional tetrahedral one [13].

As possible mechanisms contributing to decay of Mg-X donors, we assume: (i) electron-phonon interaction with multi-phonon assisted scattering; (ii) damping via vibrational modes inherent to the atoms bonding interstitial Mg atoms; (iii) defect-induced lattice disorder.

Multi-phonon cascades, even at spectral resonances to electronic energies, are generally considered to be slower processes than single-phonon-assisted electron recombination, while spectrally close local modes are considered to be potential strong enhancers of dephasing [14].

Note that molecular complexes made by abundant defects lighter than a silicon host (H, C, N, O atoms) exhibit local vibrational modes (LVM) with the largest energies exceeding the largest energies of vibrational modes in a host lattice. This extends the energy span of a potentially effective, first-order interaction of a molecular donor if impurity atoms bond into a silicon lattice via such defects.

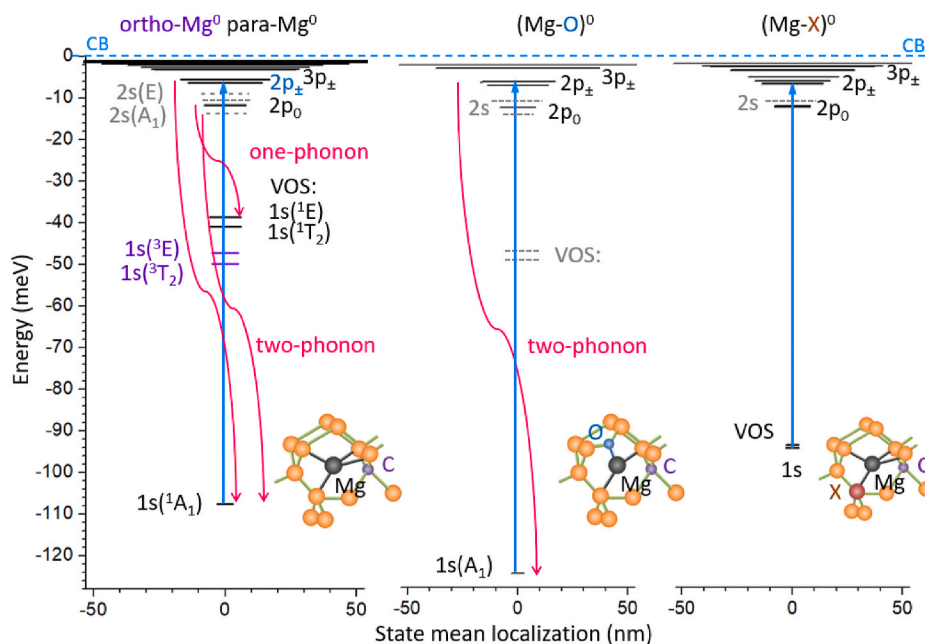


Fig. 1. Schematic presentation of the energy spectra of Mg-related double donors in silicon: (left) a neutral Mg^0 interstitial donor center; (center) a neutral $(\text{Mg-O})^0$ donor; (right) a neutral $(\text{Mg-X})^0$ donor, X stays for unknown defect [6]. Arrows upwards show typical infrared resonant excitations of centers probed in this study. Arrows down show some possible effective relaxation steps for electron decay from the probed donor states. VOS states are determined to date for Mg^0 (both para- and ortho-) [18] and for $(\text{Mg-X})^0$ donors (VOS < 1 meV); not yet determined for $(\text{Mg-O})^0$ donors (shown dashed). Not yet determined 2s states are shown by dashed lines. The graphical insets represent the hypothetical bonding structures of molecular donors as proposed by different authors: Mg at a tetrahedral interstitial position [19]; interstitial Mg_i atom bound to an interstitial Oxygen (O_i) defect; interstitial Mg_i bound to a substitutional defect X_s (e.g. metal or Mg_s [20]). Carbon (C_s) is an inherent substitutional defect. (For interpretation of the references to colour in this figure legend, the reader is referred to the Web version of this article.)

(i) First-order intervalley-phonon-electron interaction has been approved (experimentally, e.g. Ref. [15] and theoretically, e.g. Ref. [16]) to be the main mechanism that determines donor state decay at low lattice temperatures in silicon doped by substitutional atomic-like centers. Low-energy steps are maintained with assistance of acoustic intravalley phonons. Relaxation over the large-energy steps is dominated by interaction with intervalley phonons, having the energies between 11 meV and 63 meV; the maximum energy of the phonon in silicon (the zone-centered longitudinal transverse phonon, LTO) ~ 64.47 meV [17], completes the first-order phonon-electron interaction.

The largest interstate energy gaps of double Mg-X donors, between the valley-orbit-split (VOS) states and the 1s ground state or between the deepest p-type and the VOS states, exceed the LTO phonon energy for (Mg-O)⁰ centers (Fig. 1). This eliminates one-phonon-assisted processes for decay into the ground state of Mg-related donors. Since other decaying processes, including the second-order, two-phonon-assisted, were considered to be ineffective, double donors were expected to have long-living excited states.

(ii) Chemical structures of double Mg-X donors are unknown at present. There are several hypotheses based on different experimental observations and various interpretations.

Mg-O double donors are regularly observed in infrared absorption spectra of Czochralski-grown Cz-Si:Mg, where concentration of interstitial oxygen exceeds 10^{16} cm⁻³ [21]. Interstitial oxygen occurs to be an effective trap (final destination) for “mobile” Mg_i atoms, obviously weaker coupled to their “original” (as diffused) sites: such a long-term (up to three years after the diffusion) migration was followed by consequent impurity absorption spectra [22,23]. This allows one to consider a Mg_i-O_i complex to be formed by sticking a Mg atom to an oxygen center (inset in Fig. 1, center); the latter occupies its conventional interstitial position between two silicon atoms [24]. The distinguished feature of an oxygen defect in silicon is its LVM with the energy spectrum span from 29 cm⁻¹ to 1736 cm⁻¹ (3.6–215.2 meV) [25]. The lifetimes of the most intense O_i asymmetric stretch modes are 11.5 ps (¹⁶O) and 4.5 ps (¹⁷O) respectively, with an assumed decay into the TO + TO + TA combinations of the silicon modes [26]; other modes exhibit about the lifetimes in the same order if one compares the linewidths of its infrared-active transitions, e.g. the lifetimes of the oxygen-related modes within the energy gap of interest (517-648 cm⁻¹, 64–80 meV [23]) can be estimated as around 2 ps. Additionally, oxygen-carbon LVMs have been found in Cz-Si crystals, where O_i-C_s LVMs include those in the mid-infrared: 91.7 meV; 107.2 meV; etc [27].

Mg* double donors are observed in the absorption spectra of Si:Mg crystals whose Mg⁰ densities are larger than 10^{14} cm⁻³ [28]. There is no yet a common view on the unknown atom(s) in this Mg-X molecule. The original idea [20] was that this center might be a Mg_i-X_s complex, while X could be a transition metal, acceptor center, or even Mg_s at substitutional site, not excluding multiple atomic configurations. Later, this center was explained as either Mg_i inhabiting an alternate interstitial site, or Mg_i complexing with other unknown species [6]. The very small VOS of Mg*, found in absorption spectroscopy [6], could suggest both these interpretations. For the case of a molecular-type Mg-X complex, its forming species X should probably be light atom(s); note that substitutional carbon is the next possible candidate—typical carbon concentrations in the studied crystals, where Mg* were detected, are above 10^{14} cm⁻³. High long-term chemical stability of Mg* centers in Si:Mg samples could indicate a chemically stable X host (inset in Fig. 1, right). While infrared-active C_s-LVM are observed in the absorption spectra: 70.9 meV; 72.6 meV; 86 meV [29], determination of its lifetime is challenging because of the strong background due to the overlapping strongest two-phonon absorption band. It can be alternatively estimated from the theoretically predicted C_s-LVM IR-linewidth at 596 cm⁻¹ (73.9

meV) [26], to be ~ 0.64 ps.

(iii) The comprehensive technologic study of diffusion doping of Mg in silicon, showed that only a small portion (below 1 %) of the diffused Mg occupies the sites forming electrically active Mg⁰ donors [30], the lesser part may form Mg-X centers, depending on diffusion conditions and defects in the original Si crystal, while the rest of Mg occurs to be electrically inactive and not detected by optical analytical spectroscopies [23]. While concentration broadening of donor states has not been safely experimentally verified to influence electronic relaxation in low-to-moderately-doped silicon, concentrations of defects above a ppm level cause a measurable lattice disorder, as for instance those detected in properties of substitutional hydrogen-like donors in silicon [31]. Typical uncertainties in the level energies at such concentration of defects, converted by the uncertainty principle to the lifetime values are in the order of a few ps.

According to impurity absorption and electron paramagnetic resonance spectra, a neutral Mg⁰ center (Fig. 1, left) is classified as a double donor on its interstitial tetrahedral site [13,19] (inset in Fig. 1, left). The energies of ground-state-split-off para- and ortho-states [18] can serve as intermediate states or electron traps in nonradiative relaxation processes. Dynamics of Mg⁰ excited states in silicon was revisited by complementary time-resolved spectroscopic techniques and revealed relatively short, tens of ps, time scales, different from the earlier predicted in Ref. [11], assuming a first-order-phonon coupling to Mg states. Efficient one-phonon coupling can be expected only between 2p₀ and VOS states, two-phonon overtones are quasi-resonant to the energy gap between 2p_± and the ground states. Additional two-phonon resonances could occur between 2s and 1s states, but the binding energies of 2s states remain undetermined till present.

The VOS of a Mg-O donor is not known to date: there are arguments, following the estimates of a Mg-O ground state radius [28], that its trend for the VOS to the chemical shift may be similar/close to those for a Mg⁰ center. The distinguished feature of an oxygen defect is clearly observed (Fig. 2a) through its most intense series of a¹⁶O isotope.

Similar to a Mg atomic center, there are (two-phonon) overtones quasi-resonant to the energy gap between 2p_± and ground states. Additional two-phonon resonances could occur between 2s and 1s states, the binding energies of 2s states of Mg-O have not yet been determined.

No one-phonon coupling can be foreseen between the deepest Mg-O states on the basis of current knowledge of its energy spectrum.

Mg* (Mg-X) centers have no resonances to both one-phonon and to overtones, for the energy between the deepest excited states of a Mg* center. The combinational two-phonon interaction may couple the higher excited states (3p_± and higher).

3. Experimental

3.1. Samples

The Si:Mg samples in this study are the heritage of the former long-term cooperation between the Ioffe Institute, St. Petersburg, Institute for Physics of Microstructures, N. Novgorod, Leibniz-Institut für Kristallzüchtung (IKZ) and DLR Institute of Optical Sensor Systems in Berlin. The technology of the crystal growth, doping and samples manufacturing is described in details elsewhere, see e.g. the Review [23] and References therein. All crystals have the grown axis (001) which is kept as the sample optical axis; the large, polished facets are wedged to the opposite. For the crystals containing Mg-O centers, a CZ-grown (oxygen concentration $\sim 5 \times 10^{17}$ cm⁻³) initially undoped silicon was used, while the crystals containing Mg* centers were made from a float-zone-grown (FZ) Si with residual acceptors at $\sim 6.2 \times 10^{12}$ cm⁻³. Concentration of formed Mg⁰, (Mg-O)⁰ and (Mg*)⁰ donors were

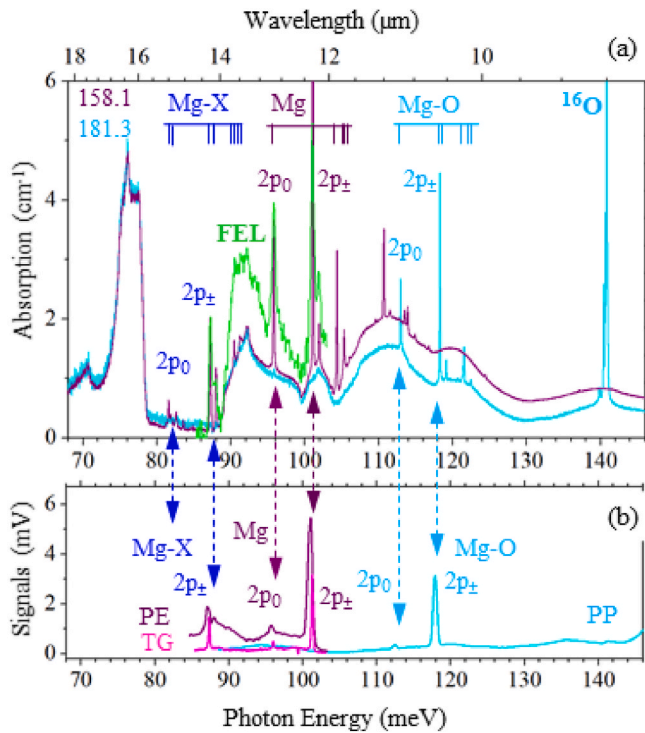


Fig. 2. (a) Infrared absorption spectra of magnesium-doped silicon samples, containing atomic Mg donors and molecular Mg-X (Si:Mg #158.1) and Mg-O donors (Si:Mg #181.3). Note the two- and three-phonon absorption bands forming the background infrared absorption in this spectral region. Shown in green: FEL absorption spectrum in the region of the Mg⁰ donor transitions. (b) Typical FEL wavelength-scan spectra of these samples show the peak intensity of photon echo, transient grating (Si:Mg #158.1) and pump-probe (Si:Mg #181.3) responses. The arrows indicate the FEL photon energy used to pump the samples; note the slight discrepancy between the spectra recorded by linear absorption (Fourier transform) and those obtained with the FEL dispersive analyzer. The impurity absorption transitions exhibit much broader linewidths (see also Refs. [6,28]) than the transition linewidths of hydrogen-like single-electron donors in samples of similar concentration [36]. This suggests relative short lifetimes of Mg-related donors. (For interpretation of the references to colour in this figure legend, the reader is referred to the Web version of this article.)

estimated on the basis of their optical characterization using the calibration factors obtained in Ref. [28], oxygen and carbon – using the calibration factors as in Ref. [31].

A 2.3 mm-thick 1.5°-wedged Si:Mg #158-1 sample has $\sim 1.8 \times 10^{14} \text{ cm}^{-3}$ of Mg* centers and $\sim 1.5 \times 10^{15} \text{ cm}^{-3}$ Mg⁰, and residual lithium at $\sim 5.7 \times 10^{13} \text{ cm}^{-3}$. A 1.8 mm-thick 1.5°-wedged Si:Mg #181-3 sample has $\sim 5 \times 10^{14} \text{ cm}^{-3}$ of Mg-O centers with residual (lower than 10^{13} cm^{-3}) Mg⁰, Mg-B and Li-O donors.

3.2. Characterization of molecular-type Mg-related centers in silicon

Infrared absorption spectroscopy at low temperature was used to assess the abundances of different type Mg-related donors in silicon crystals grown and doped by Mg in order to obtain the sample containing Mg-O (Czochralski-grown) and Mg-X (float-zone grown) double donors. The impurity spectra were taken at low temperatures ($\sim 5 \text{ K}$) using a Bruker Vertex 80v Fourier transform IR spectrometer equipped with different detectors for the far-infrared (Si bolometer) and the mid-infrared (pyroelectric DLaTGS (Deuterated L- α Alanine doped TriGlycine Sulphate) detectors) covering the spectral range from 1 meV to 1 eV. The typical spectral resolution was 0.13 cm^{-1} (photon energy of 16 μeV). The samples were glued with a silver paint to a cold finger in a liquid-He flow cryostat (SuperTran, Janis Research), and cooled down

to $\sim 5 \text{ K}$. The temperature was monitored by calibrated sensors (Lake Shore) mounted on a cold finger in the vicinity of the sample. Infrared absorption was calculated using a simplified approach of a single-path propagation of the light through a wedged sample.

The impurity absorption spectra of molecular Mg-donors (Fig. 2a) consist of similar types of the $s \rightarrow p$ transitions series between the center's ground state and the excited states, with the most intense lines terminating in the deepest p-type excited states. The amplitude of unsaturated absorption lines was used for the determination of impurity partial concentrations. Empirical transmission values at impurity transitions were used for simulated decay functions when using multi-level modelling.

To date, continuous wave linear infrared spectroscopy of shallow impurity centers in silicon could resolve the impact of impurity-phonon interaction on the relaxation of the excited impurity state only for cases where the excited-to-ground state transition are resonant with the energy of a single optical phonon in silicon: the zone-centered longitudinal transverse phonon (LTO) in p-Si:Al, p-Si:Ga [32] and the intervalley transverse g-TO phonon in n-Si:Bi [33]. Such resonances cause either a strong broadening of the corresponding impurity transition or its disappearance in the absorption spectrum.

Large chemical shifts of the ground states of double donors move intracenter transitions into the high-order-phonon bands, some of which are infrared active. The resonances of the ground-to-excited transitions of molecular Mg-related centers can only be found with two-phonon and three-phonon bands [34]. The transitions of neutral (Mg-O)⁰ centers overlap spectrally with the two-phonon absorption bands in silicon [34, 35], similar to a neutral Mg⁰ center; this is not the case for the low-frequency transitions of a neutral Mg-X (Mg*)⁰ center (Fig. 2a). Spectra of oxygen-LVMs overlap with one-, two-, and three-silicon phonon bands. The strong lines of ¹⁶O LVM (Fig. 2a) are regularly used to estimate the concentration of O_i.

3.3. Time-resolved spectroscopy

Transients in a single-frequency pump-probe (PP), photon echo (PE) and transient grating (TG) modes have been studied using the dedicated time-resolved spectroscopy setup in the FELIX lab, see for more details [11] and Supplemental materials.

The FEL emits near bandwidth-limited, few ps pulses with a narrow spectral bandwidth (typically below 0.5 %). The laser bandwidth determines the time resolution of the techniques which varied in our experiments between 2.4 and 3.5 ps. We used a repetition rate of 25 MHz for micropulses which fill about 10 μs -long macropulses coming at 10 Hz repetition rate. All time-resolved techniques, provided in this setup, require the splitting of the incident beams with pellicle beam splitters. Temporal delays necessary to record sufficient decay dependences, up to 1 ns, in incoming pulses, are provided by mechanical delay stages with the step accuracy of about 1 μm .

The pump beam incidence is set normal to the sample front faced, and has a polarization parallel to a [110] direction of a Si:Mg sample. The other beams are declined by about 5° with respect to the pump beam. The spot size of all beams is about 2 mm.

A liquid-helium cooled Ge:Ga detector receives either transmitted or diffracted probe pulses (PP and TG spectroscopies) or photon echo pulse. The two latter beams are acquired in the phase respective matching directions. The samples were glued by silver paint to a cold finger in a liquid-helium-flow cryostat, and cooled down to $\sim 3.5 \text{ K}$.

We measured transients over the spectral regions covering the most intense intracenter transitions of a particular donor: these are regularly the transitions between the ground state and the deepest excited p-type states, $2p_0$ and $2p_{\pm}$ (Fig. 2b). Pumping off-resonance to the impurity transitions was used to obtain other accompanying contributions. Note that infrared-active two-phonon bands as well as local vibrational modes do not exhibit their own characteristic PP, PE, TG signals (Fig. 2b).

The time dependences PP(t), PE(t), TG(t) obtained for the molecular

donors Mg-X were compared with the data when pumping in the similar ($2p_0$ and $2p_{\pm}$) Mg^0 states. The pump-probe evolutions were recorded in two different polarizations of the probe beam relative to the pump beam: parallel ($\text{PP}0^\circ(t)$) and orthogonal ($\text{PP}90^\circ(t)$).

Results of the fits of the transient evolution by different models are collected in the Supplemental materials. We further discuss the validity of using different fitting functions for the decay slope of the measured temporal dependences: a simple single-exponential decay and a multi-level formalism, see Table 1 and Supplementary materials for further details.

4. Results

4.1. Photon echo

Photon echo (PE) detection is a standard tool of nonlinear spectroscopy for determining the dephasing time of macroscopic electric dipole moment, resonantly optically excited in the medium: in our case of intracenter pumping, a probed state is the excited impurity state.

In a general view of the decay of the resonantly excited oscillatory dipole moment, the photon echo decay can be evaluated with a single-exponential decay function. The echo decay rate W_{PE} is then the sum of the depopulation rate of the excited state W_1 and the homogeneous phase relaxation W_2^{hom} [37].

Analysis of the temporal PE dependences (Fig. 3) shows the validity of such fits (see Supplemental materials for more details). The dephasing decay constants determined by fitting the $\text{PE}(t)$ under excitation of the $2p_0$ and $2p_{\pm}$ donor states of all Mg-related centers are less than 10 ps; with the shortest times T_{PE} for atomic Mg^0 centers, while they are the longest for molecular $(\text{Mg-O})^0$ centers. Because of the weak PE signal when pumping into the $2p_0$ state of Mg^* molecular donors, an accurate determination of the characteristic decay is not possible.

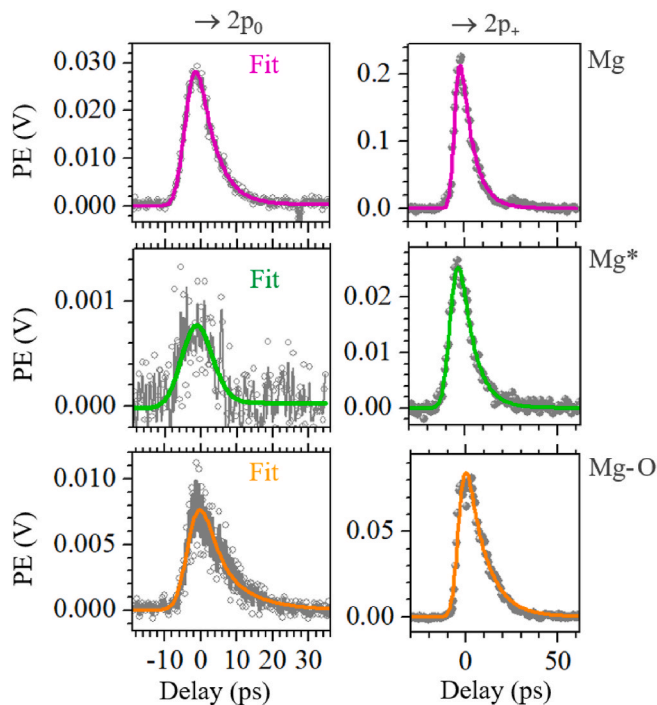


Fig. 3. Photon Echo decay when pumped into $2p_0$ and $2p_{\pm}$ states of Mg-related donors. For the weak PE signals which become close to the SNR/LOD, we add B-spline lines connecting the PE experimental data points, for better visibility. Fitting functions shown are the full-time span functions S2.

Photon Echo decay constants, T_{PE} , ps (assuming a FEL Gaussian pulse shape)

! stands for signal-to-noise and time-resolved-limited.

probed state	Mg	Mg*	Mg-O
$2p_0$	4.6	1.4 !	8
$2p_{\pm}$	7	8	14

Photon Echo decay rates, W_{PE} , ps^{-1} (fitting the decaying slope only, single-exponential function)

probed state	Mg	Mg*	Mg-O
$2p_0$	0.21 ± 0.01	0.25 !	0.12 ± 0.01
$2p_{\pm}$	0.155 ± 0.015	0.134 ± 0.005	0.11 ± 0.01

These characteristic dephasing times, derived from the fits of $\text{PE}(t)$, are several times shorter than those reported for an isocoric substitutional atomic donor in silicon [38].

4.2. Transient grating

Transient grating (TG) detection is an elegant time-resolved tool of nonlinear spectroscopy for determining the depopulation time T_1 of the electric dipole moment, optically resonantly excited in the medium. In our case of intracenter pumping, the probed state is the excited impurity state. In this four-wave mixing technique, two optical pump pulses cross in the sample to generate a spatially periodic TG, its dynamics is monitored by detection of a probe pulse diffracted from the TG (Fig. 4 inset). TG signals are virtually free of scattered light – the main source of background signal in pump-probe experiments.

The far-infrared wavelength range is not favorable for this technique because of inherently (laser spot) limited number of TG periods per unit

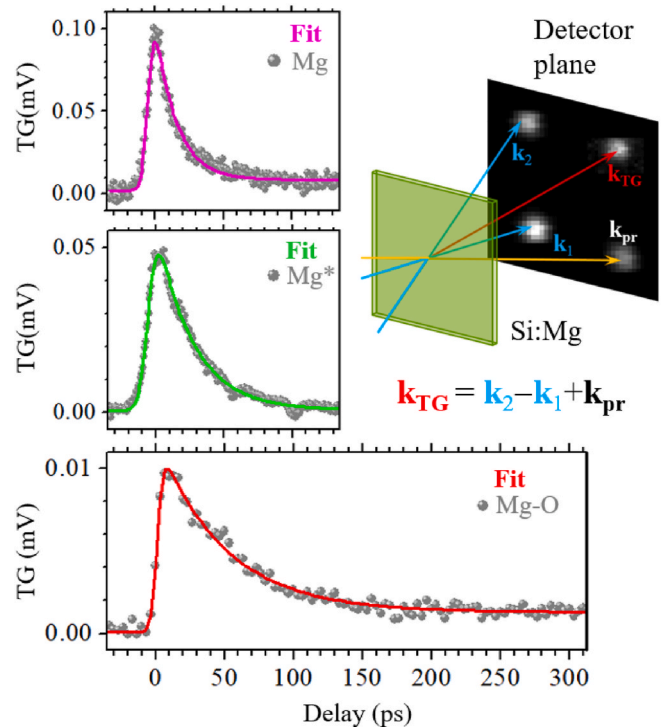


Fig. 4. Transient grating dependences taken under resonant excitation into the excited $2p_{\pm}$ state for different neutral donors: Mg, Mg-O and Mg^* . Inset depicts a scheme of optical beams: k_{pr} stays for the probe beam and k_2 and k_1 for the pump beams forming a grating. Angles: between pump beams about 5° , and between pump 1 and probe is about 5° . Resulting $k_{\text{TG}} = k_2 - k_1 + k_{\text{pr}}$ is the direction where the diffracted transient is found.

length, which could be induced in the sample. This diminishes the intensity of the diffracted light.

In our case of intracenter pumping, the TG evolution replicates the absorption dynamics at the frequency of the excited impurity transition, i.e. mainly the population difference between pumped and ground states of the donor centers [11]. The state populations can be estimated in simple multi-level models (two-level (2LS), three-level (3LS)), similar to the approach used in Ref. [39]. The decay rate of the pumped state W_1 , obtained from the modeling, defines its depopulation time T_1 .

Fig. 4 shows a typical evolution of TG transients when Si:Mg is pumped to the $2p_{\pm}$ state, for the molecular Mg-X centers, compared to the values measured for an atomic Mg donor.

The fitting by the (S1) function return the following decay time constants: 15 ps (Mg); 25 ps (Mg^*) and 50 ps (Mg-O).

The analysis shows that TG(t) for the atomic Mg $2p_{\pm}$ state can be fitted with almost the same accuracy by the three-level model, which assumes parallel cascade decay $3 \rightarrow 2 \rightarrow 1$ and direct $3 \rightarrow 1$ relaxation, with either direct relaxation dominating (this constrains the decay rate of the pumped state to $W_1 \sim 0.083\text{--}0.087 \text{ ps}^{-1}$) or the faster cascade decay (in these models, the decay rates of the upper state become dependent on the lifetime of the intermediate state and lie in a relatively wide range, $0.12\text{--}0.20 \text{ ps}^{-1}$ with the best accuracy for the rates around $W_1 \sim 0.18 \text{ ps}^{-1}$). The two-level model provides a slightly worse accuracy than the 3LS models by fitting.

The TG(t) evolution for the Mg^* molecular $2p_{\pm}$ state is fairly described by the two-level model with the rate W_1 of about 0.037 ps^{-1} . Roughly equally good fits using three-level models give the relaxation of the upper state $W_1 \sim 0.046\text{--}0.053 \text{ ps}^{-1}$ for the fast, direct decay scenario and $W_1 \sim 0.069\text{--}0.081 \text{ ps}^{-1}$ for the faster cascade via an intermediate state.

Similar trends hold for TG(t) for the Mg-O $2p_{\pm}$ state: a two-level system with rate W_1 of about 0.021 ps^{-1} seems to be sufficient for high accuracy fits. Alternative three-model fits yield either a fast, direct relaxation with the upper state decay rate within $W_1 \sim 0.027\text{--}0.030 \text{ ps}^{-1}$, while faster cascade scenarios require rates either within $W_1 \sim 0.025\text{--}0.029 \text{ ps}^{-1}$ (short-living intermediate state) or $W_1 \sim 0.036\text{--}0.043 \text{ ps}^{-1}$ (short-living upper state).

4.3. Pump-probe spectroscopy

Pump-probe spectroscopy is a standard time-resolved tool for determining the dynamics of the populations of electronic states involved in light absorption, emission and in nonradiative processes. For any medium with electronic spectra involving more than two levels, multiple levels can contribute to the above processes; this requires a valid analysis of the observed PP(t). More intense responses (compared to PE and TG techniques) enable additional insights into the weaker processes involved in the relaxation of nonequilibrium carriers, such as cascade decays and/or pump-induced light absorption.

The inherent weakness of the single-frequency pump-probe technique is often collateral contributions unrelated to the probed electronic states and/or leak/scattering of pump light into the probe optical path. The most challenging for interpretation is often the time interval around time zero – the time when pump and probe beam overlap.

The PP evolution under pumping into the $2p_0$ state of all Mg-related donors reveals a complex evolution of the probe transmission (Fig. 5) that cannot be explained by a two-level system. The specific feature of the PP(t) is the occurrence of the fast component, and in both relative polarizations of the pump and probe beams. Large difference in the characteristic times, that could describe such a slope, implies the three-level model with a much faster direct decay channel ($W_{31} \gg \{W_{32}, W_{21}\}$).

The PP(t) under pumping into $2p_{\pm}$ states exhibits almost monotonic decay (Fig. 6). The longest times are found for the PP(t) of a Mg-O center, while the difference between molecular and donor centers is smaller if compared to those for the decay of $2p_0$ states.

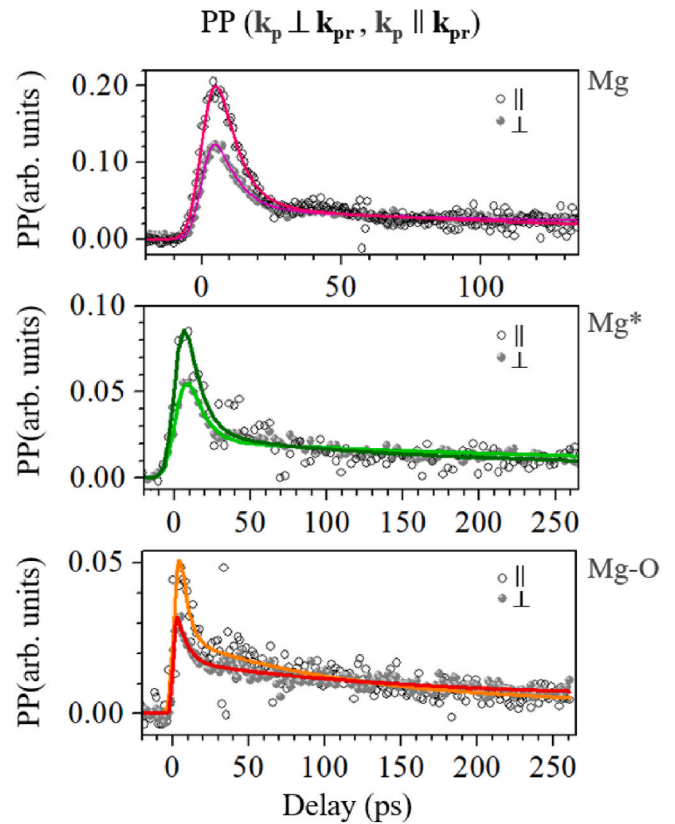


Fig. 5. Pump-probe dependences under resonant excitation into the $2p_0$ state for neutral donors: Mg, Mg^* and Mg-O taken under two different relative polarizations of a probe beam: parallel and orthogonal to a pump beam. The (S1) model approaches used to fit $PP^{\circ}(t)$ are shown as solid lines in the plots, for the 3LS fitting of the decay slope part please see Supplemental materials.

This could be a consequence of quasi-resonances between interstate transitions and phononic overtones. The fast components in the sum of the exponential functions of molecular centers are about twice as long as those of PE(t).

For Mg atomic centers, the fast, direct decay scenarios for the $2p_0$ state result in the following rates for relaxation of the pumped state under parallel probe and pump beams:

$W_1 \sim 0.10\text{--}0.13 \text{ ps}^{-1}$ (short-living intermediate state) or $W_1 \sim 0.12\text{--}0.14 \text{ ps}^{-1}$ (short-living upper state). At such rates, less than 1 % of the excited carriers pass through the intermediate state, and hence one can consider a fast, single-step decay process as the dominant relaxation process of the $2p_0$ state in Mg centers. The depopulation rate of the pumped state appears to be about half the decay rate for its photon echo.

Faster cascade decay schemes yield poorer quality fits, with the corresponding rates of the upper state decay $W_1 \sim 0.10\text{--}0.14 \text{ ps}^{-1}$ (short-living intermediate state) or $W_1 \sim 0.15\text{--}0.16 \text{ ps}^{-1}$ (short-living upper state).

The $PP^{90^{\circ}}(t)$ at orthogonal polarization give very similar results in time constants and trends, see Supplemental materials for details. The relatively larger slow component in $PP^{90^{\circ}}(t)$ would require the larger contribution of the cascade channel to the total decay of the $2p_0$ state, however, it does not exceed $\sim 2\%$, and by this, can also be considered as a minor relaxation path.

The intermediate state can be considered as a non-vanishing contributor to the decay of the nonequilibrium population of the $2p_0$ state of atomic Mg centers.

The best fits to PP(t) of the Mg $2p_{\pm}$ state under parallel and also orthogonal probe and pump beams are fast cascade pathways. In these schemes, the decay rates of the pumped state are about $W_1 \sim 0.16\text{--}0.19 \text{ ps}^{-1}$ and the decay rate of the intermediate state is the slowest process

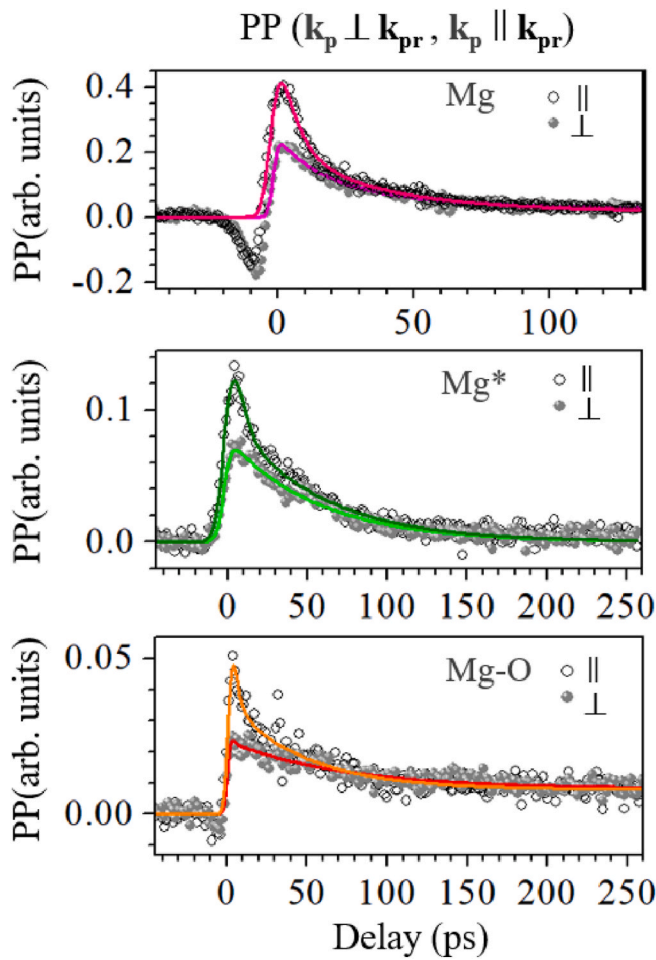


Fig. 6. Pump-probe dependences under resonant excitation to the $2p_{\pm}$ state for neutral donors: Mg, Mg* and Mg-O, recorded for two different polarizations of the probe beam: parallel and orthogonal to the pump beam.

$\sim 0.03 \text{ ps}^{-1}$, i.e. cannot be uniquely assigned to the $2p_0$ state. If we recall that the cascade part of the relaxation of the Mg $2p_0$ state contains an option with approximately the same rate (Supplemental materials), a common intermediate state can contribute to the relaxation of both $2p$ -type states of atomic Mg centers. Similar rates were estimated for the cascade decay via the VOS states in Ref. [40].

Pump-probe measurements of the $2p_0$ state of a Mg* center do not resolve the faster channel, apparently because of the low accuracy of the PP(t) around time zero, for a very fast component. For parallel beams, both the fast cascade (W_1 for this scenario $\sim 0.16\text{--}0.18 \text{ ps}^{-1}$) and the fast, direct relaxation (with W_1 for this scenario $\sim 0.079\text{--}0.085 \text{ ps}^{-1}$) provide fits with the same accuracy; slightly worse is the fit of the 2LS model. For orthogonal beams, only the fast, direct relaxation in the 3LS model gives an accurate fit, while the relaxation rate for the pumped state in this scenario is very high: $W_1 \sim 0.19\text{--}0.20 \text{ ps}^{-1}$.

A fast component is not noticeably expressed in the PP(t) of a $2p_{\pm}$ state of a Mg* center. 3LS models with a fast cascade yield a decay rate of the pumped $2p_{\pm}$ state $W_1 \sim 0.09\text{--}0.10 \text{ ps}^{-1}$ (parallel beams) or $W_1 \sim 0.07\text{--}0.08 \text{ ps}^{-1}$ (orthogonal beams). Other alternative schemes yield a much slower rate of the pumped $2p_{\pm}$ state $W_1 \sim 0.04\text{--}0.06 \text{ ps}^{-1}$. The rate for an intermediate state W_{21} is held around $\sim 0.02 \text{ ps}^{-1}$, which is far from the values determined for the relaxation of the $2p_0$ Mg* state.

The common relaxation scheme of the $2p_0$ state of a Mg-O center for parallel and orthogonal polarizations is a fast, direct decay in a 3LS model. The depopulation rates of the pumped state are then $W_1 \sim 0.12\text{--}0.13 \text{ ps}^{-1}$ (parallel beams) or $W_1 \sim 0.14\text{--}0.16 \text{ ps}^{-1}$ (orthogonal beams).

Pump-probe dependences of the $2p_{\pm}$ state of a Mg-O center at different polarization do not give common results: PP(t) at orthogonal polarization does not require an intermediate state to explain its evolution. Alternative 3LS models give rates $W_1 \sim 0.030\text{--}0.035 \text{ ps}^{-1}$; while PP(t) for parallel beams have good fits only within 3LS models, with W_1 rates between 0.063 ps^{-1} and 0.085 ps^{-1} . In the latter fits, the decay rate of an intermediate state would require $\sim 0.020 \text{ ps}^{-1}$.

5. Conclusions

Time-resolved spectroscopies of Mg-related molecular donors, Mg-X, reveal very short dephasing time of the deepest excited states, which are reflected in the photon echo decay times, within 7–9 ps (Table I). These times, however, are even longer than the photon echo decay constants of an atomic Mg donor, which range between 4.6 ps and 7.0 ps. The observed times are about three times shorter than those reported for single-electron donors [38]. High decay rates of the pumped $2p_0$ state of molecular Mg-O and Mg* centers as well as the $2p_{\pm}$ state of a Mg center can explain the dephasing of this state solely by state depopulation alone, other states of the donors would then require additional mechanisms.

All dephasing times are in close vicinity to the times that could be derived from the spectral linewidths of the respective intracenter absorption transitions, assuming their line broadening to be lifetime-limited.

Note that there is no regular correlation between the times measured in PP(t) at different polarizations.

One could argue about an existing overlap of rates for a pumped $2p_{\pm}$ state, as determined by the analysis of transient grating and pump-probe techniques. This fact can be used to constrain some relaxation pathways.

For instance, the relaxation of the $2p_{\pm}$ state in atomic Mg⁰ centers is most likely dominated by a faster cascade. As discussed above, the intermediate state of such a cascade is unlikely to be a $2p_0$ state, as is commonly expected for shallow, single donors in silicon [16]. The common states in the relaxation of the both deepest p-type states are apparently the 1s-type VOS states. In these processes, the relaxation steps could be due to first-order phonon-assisted processes.

For the measured relaxation of atomic acceptors in silicon, it has been argued that the intracenter relaxation rates follow the phonon density of states [41]. We find no such correlation when comparing the observed times/rates with the theoretically derived values [42], nor when comparing between states of the same center or the same transition of different centers (Table I).

Similarly to atomic centers, the $2p_{\pm}$ state in molecular Mg⁰ centers can be dominated by a faster cascade. However, a fast, direct decay scenario remains a plausible alternative with about the same quality of the relaxation model to the experimental PP(t) evolution. Here, we can exploit the knowledge of the Mg* center energy spectrum and the obtained decay rates of the $2p_0$ state, which is too high to be assigned as an intermediate state for relaxation from the $2p_{\pm}$ state. This constrains the possible relaxation pathways to either the $2p_{\pm} \rightarrow 2s \rightarrow 1s(A_1)$ cascade (similar to those proposed for an arsenic donor in silicon [43]) and/or the direct $2p_{\pm} \rightarrow 1s(A_1)$ decay. Both require a large energy step and therefore act like a two-phonon accompanying process, which obviously occurs at a very high rate, $W_1 > 46 \text{ ns}^{-1}$. The $2p_0$ state of a Mg* center exhibits a dominating direct decay to the ground state with a rate $> 160 \text{ ns}^{-1}$. This fits well to the inverse linewidth of the Mg* absorption transition $2p_0 \rightarrow 1s(A_1)$.

However, such a fast decay of a Mg* center does not follow its state energy spectrum, which has no evident resonances to single or sum phonon energies. Therefore, alternative to lattice phonon accompanying relaxation and dephasing mechanisms should likely contribute to the dynamics of Mg* centers.

Similarly to Mg* centers, the $2p_{\pm}$ state in Mg-O centers decays slowly compared to its $2p_0$ state. The common rate W_1 for both polarizations in pump-probe and in transient grating experiments results points direct

Table 1

Decay times of Mg-related double neutral centers derived/constrained from the evolution of transients recorded by different time-resolved spectroscopies (ps) and decay rates evaluated by different models. The beam polarizations: (||) parallel; (⊥) orthogonal. The calculated data for two-phonon density of states (TDOS) in silicon [42] are given.

Neutral Donor	state	Time-resolved spectroscopy						Line	Phonon
		PE		TG		PP			
		T _{PE} (ps) S1	W _{PE} (ns ⁻¹)	T _{TG} (ps) S1	W ₁ (ns ⁻¹)	T _{PP} (ps) or ⊥ S1	W ₁ (ns ⁻¹) or ⊥ or both		
Mg	2p _±	7	155 ± 15	15	63 ± 5 ²⁾ 83–87 120–200	10 32 ⊥	160–190	11	0.055
	2p ₀	4.6	210 ± 10			9 10 ⊥	100–130 120–140	9.6	0.037
Mg ^a	2p _±	8	134 ± 5	25	37 ± 1 ²⁾ 46–53 69–81	4, 45 60 ⊥	25 ± 1 ²⁾ ⊥ 40–60 70–80 ⊥ 90–100	11.4	0.017
	2p ₀	1.4!	<250 !			3, 111 3, 44 ⊥	79–85 160–180 190–200 ⊥	5–11.8 ^a	0.071
Mg-O	2p _±	14	110 ± 10	50	21 ± 1 ²⁾ 27–30 25–29 36–43	6, 54 4.5, 113 ⊥	15 ± 1 ²⁾ 40 ± 2 ²⁾ ⊥ 30–35 ⊥ 63–85	11.4	0.083
	2p ₀	8	120 ± 10			5, 115 8, 183 ⊥	120–130 140–160 ⊥	11.3	0.038

! signal-to-noise limited.

²⁾ 2LS model, without index: 3LS models.

^a Different components.

decay as the main mechanism in the 2p_± state relaxation, the obtained rate is W₁ > 30 ns⁻¹. The 2p₀ state of a Mg-O center has a dominating direct decay to the ground state with a rate >120 ns⁻¹. A large energy gap to the ground state would imply a two-phonon relaxation process. The fast depopulation rates of the 2p_± and 2p₀ Mg-O states could be linked to their resonances to phonon overtones and sum frequencies.

Resuming the above, second-order electron-phonon interactions, requiring multiple phonons for energy conservation, remain the main plausible processes for the decay of molecular Mg-related donors in silicon. This impurity-multi-phonon interaction appears to be almost as fast as first order processes – this is in contradiction to the predictions previously made for deep donors in silicon [39]. The optical phonon overtones were considered to be effective mediators for electronic decay in double donors in silicon [40].

The question about the possible influence of LVM on the dephasing of molecular Mg-related donors in silicon remains open.

CRediT authorship contribution statement

S.G. Pavlov: Writing – review & editing, Writing – original draft, Validation, Supervision, Investigation, Formal analysis, Data curation, Conceptualization. **N. Defmann:** Writing – review & editing, Validation, Resources, Methodology, Investigation, Formal analysis, Data curation, Conceptualization. **N.V. Abrosimov:** Writing – review & editing, Resources, Methodology, Investigation.

Acknowledgements

Authors acknowledge the FELIX Laboratory for providing the beam time. We thank Prof. B. N. Mordin for fruitful discussions and the group of Dr. Yu. Astrov for technical support.

Appendix A. Supplementary data

Supplementary data to this article can be found online at <https://doi.org/10.1016/j.mssp.2025.110158>.

Data availability

Data will be made available on request.

References

- [1] J.-P. Connerade, Quasi-Atoms and super-atoms, *Phys. Scri.* 68 (2003) C25, <https://doi.org/10.1238/Physica.Regular.068aC0025>.
- [2] H.J. Queisser, E.E. Haller, Defects in semiconductors: some fatal, some vital, *Science* 281 (1998) 945–950, <https://doi.org/10.1126/science.281.5379.945>.
- [3] R. Schirhagl, K. Chang, M. Loretz, C.L. Degen, Nitrogen-vacancy centers in diamond: nanoscale sensors for physics and biology, *Annu. Rev. Phys. Chem.* 65 (2014) 83–105, <https://doi.org/10.1146/annurev-physchem-040513-103659>.
- [4] Sakti Prasanna Muduli, Pareshe Kale, State-of-the-art passivation strategies of c-Si for photovoltaic applications: a review, *Mater. Sci. Semicond. Process.* 154 (2023) 107202, <https://doi.org/10.1016/j.mssp.2022.107202>.
- [5] L. Bergeron, C. Chartrand, A.T.K. Kurkjian, K.J. Morse, H. Riemann, N. V. Abrosimov, P. Becker, H.-J. Pohl, M.L.W. Thewalt, S. Simmons, Silicon-Integrated telecommunications photon-spin interface, *PRX. Quantum.* 1 (2020) 020301, <https://doi.org/10.1103/PRXQuantum.1.020301>.
- [6] R.J.S. Abraham, A. DeAbreu, K.J. Morse, V.B. Shuman, L.M. Portsel, A.N. Lodygin, Yu A. Astrov, N.V. Abrosimov, S.G. Pavlov, H.-W. Hübers, S. Simmons, M.L. W. Thewalt, Further investigations of the deep double donor magnesium in silicon, *Phys. Rev. B* 98 (2018) 045202, <https://doi.org/10.1103/PhysRevB.98.045202>.
- [7] S.G. Pavlov, Yu A. Astrov, L.M. Portsel, V.B. Shuman, A.N. Lodygin, N. V. Abrosimov, H.-W. Hübers, Magnesium-related shallow donor centers in silicon, *Mater. Sci. Semicond. Process.* 130 (2021) 105833, <https://doi.org/10.1016/j.mssp.2021.105833>.
- [8] A.D. Bandrauk, S.C. Wallace (Eds.), *Coherence Phenomena in Atoms and Molecules in Laser Fields*, Springer Science + Business Media, New York, 1992. *NATO Science Series B: vol. 287*.
- [9] S.K. Estreicher, T.M. Gibbons, Non-equilibrium molecular-dynamics for impurities in semiconductors: vibrational lifetimes and thermal conductivities, *Physica B* 404 (2009) 4509–4514, <https://doi.org/10.1016/j.physb.2009.08.102>.
- [10] “Nonradiative Recombination in Semiconductors” [V. N. Abakumov et al], Vol. 33 of the Series “Modern Problems in Condensed Matter Physics” (Elsevier 1991), and references therein.
- [11] N. Dessmann, S.G. Pavlov, A. Pohl, V.B. Shuman, L.M. Portsel, A.N. Lodygin, Yu A. Astrov, N.V. Abrosimov, B. Redlich, H.-W. Hübers, Combination of ultrafast time-resolved spectroscopy techniques for the analysis of electron dynamics of heliumlike impurity centers in silicon, *Phys. Rev. B* 106 (2022) 195205, <https://doi.org/10.1103/PhysRevB.106.195205>.
- [12] A.K. Ramdas, S. Rodriguez, Spectroscopy of the solid-state analogues of the hydrogen atom: donors and acceptors in semiconductors, *Rep. Prog. Phys.* 44 (1981) 1297, <https://doi.org/10.1088/0034-4885/44/12/002>.
- [13] J.E. Baxter, G. Ascarelli, A comparative electron-spin-resonance study of the ground state and a photoconverted metastable state of the mg+ donor in silicon, *Phys. Rev. B* 7 (1973) 2630, <https://doi.org/10.1103/PhysRevB.7.2630>.

- [14] T.N. Morgan, Capture into deep electronic states in semiconductors, *Phys. Rev. B* 28 (1983) 7141, <https://doi.org/10.1103/PhysRevB.28.7141>.
- [15] N.Q. Vinh, P.T. Greenland, K. Litvinenko, B. Redlich, A.F.G. van der Meer, S. A. Lynch, M. Warner, A.M. Stoneham, G. Aeppli, D.J. Paul, C.R. Pidgeon, B. N. Murdin, Silicon as a model ion trap: time domain measurements of donor Rydberg states, *Proc. Nat. Acad. Sci. USA* 105 (2008) 10649, <https://doi.org/10.1073/pnas.0802721105>.
- [16] V.V. Tsyplenkov, E.V. Demidov, K.A. Kovalevsky, V.N. Shastin, Relaxation of excited donor states in silicon with emission of intervalley phonons, *Semiconductors* 42 (2008) 1016, <https://doi.org/10.1134/S1063782608090030>.
- [17] K. Uchinokura, T. Sekine, E. Matsuura, Raman scattering by silicon, *Solid State Commun.* 11 (1972) 47–49, [https://doi.org/10.1016/0038-1098\(72\)91127-1](https://doi.org/10.1016/0038-1098(72)91127-1).
- [18] V.N. Shastin, R. Kh Zhukavin, K.A. Kovalevsky, V.V. Tsyplenkov, V.V. Rumyantsev, D.V. Shengurov, S.G. Pavlov, V.B. Shuman, L.M. Portsel, A.N. Lodygin, Yu A. Astrov, N.V. Abrosimov, J.M. Klopff, H.-W. Hübers, Chemical shift and exchange interaction energy of the 1s States of magnesium donors in silicon. The possibility of stimulated emission, *Semiconductors* 53 (2019) 1234, <https://doi.org/10.1134/S1063782619090197>.
- [19] L.T. Ho, A.K. Ramdas, Excitation spectra and piezospectroscopic effects of magnesium donors in silicon, *Phys. Rev. B* 5 (1972) 462, <https://doi.org/10.1103/PhysRevB.5.462>.
- [20] A.L. Lin, Electrical and optical properties of magnesium-diffused silicon, *J. Appl. Phys.* 53 (1982) 6989–6995, <https://doi.org/10.1063/1.330045>.
- [21] Yu A. Astrov, V.B. Shuman, L.M. Portsel, A.N. Lodygin, S.G. Pavlov, N. V. Abrosimov, V.N. Shastin, H.-W. Hübers, Diffusion doping of silicon with magnesium, *Phys. Status Solidi* 214 (2017) 1700192, <https://doi.org/10.1002/pssa.201700192>.
- [22] L.T. Ho, Room-temperature formation of magnesium–oxygen complex impurities in silicon, *Physica B* 302–303 (2001) 197–200, [https://doi.org/10.1016/S0921-4526\(01\)00428-8](https://doi.org/10.1016/S0921-4526(01)00428-8).
- [23] Yu A. Astrov, L. M. Portsel, V. B. Shuman, A. N. Lodygin, N. V. Abrosimov, Magnesium-related donors in silicon: state of the art, *Phys. Status Solidi*, 219: 2200463. doi: 10.1002/pssa.202200463.
- [24] H. Yamada-Kaneta, C. Kaneta, T. Ogawa, Theory of local-phonon-coupled low-energy anharmonic excitation of the interstitial oxygen in silicon, *Phys. Rev. B* 42 (1990) 9650, <https://doi.org/10.1103/PhysRevB.42.9650>.
- [25] T. Hallberg, L.I. Murin, J.L. Lindström, V.P. Markevich, New infrared absorption bands related to interstitial oxygen in silicon, *J. Appl. Phys.* 84 (1998) 2466–2470, <https://doi.org/10.1063/1.368407>.
- [26] B. Sun, Q. Yang, R.C. Newman, B. Pajot, N.H. Tolk, L.C. Feldman, G. Lüpke, Vibrational lifetimes and isotope effects of interstitial oxygen in silicon and germanium, *Phys. Rev. Lett.* 92 (2004) 185503, <https://doi.org/10.1103/PhysRevLett.92.185503>.
- [27] L.I. Khirunenko, M.G. Sosnin, Yu V. Pomozov, L.I. Murin, V.P. Markevich, A. R. Peaker, L.M. Almeida, J. Coutinho, V.J.B. Torres, Formation of interstitial carbon–interstitial oxygen complexes in silicon: local vibrational mode spectroscopy and density functional theory, *Phys. Rev. B* 78 (2008) 155203, <https://doi.org/10.1103/PhysRevB.78.155203>.
- [28] S.G. Pavlov, L.M. Portsel, V.B. Shuman, A.N. Lodygin, Yu A. Astrov, N. V. Abrosimov, S.A. Lynch, V.V. Tsyplenkov, H.-W. Hübers, Infrared absorption cross sections, and oscillator strengths of interstitial and substitutional double donors in silicon, *Phys. Rev. Mater.* 5 (2021) 114607, <https://doi.org/10.1103/PhysRevMaterials.5.114607>.
- [29] R.C. Newman, J.B. Willis, Vibrational absorption of carbon in silicon, *J. Phys. Chem. Solid.* 26 (1965) 373–379, [https://doi.org/10.1016/0022-3697\(65\)90166-6](https://doi.org/10.1016/0022-3697(65)90166-6).
- [30] L.M. Portsel, V.B. Shuman, A.A. Lavrent'ev, A.N. Lodygin, N.V. Abrosimov, Yu A. Astrov, Investigation of the magnesium impurity in silicon, *Semiconductors* 54 (2020) 393, <https://doi.org/10.1134/S1063782620040120>.
- [31] S.G. Pavlov, N.V. Abrosimov, Impurity-induced enhancement of parity-forbidden optical intracenter transitions of shallow donors in silicon, *Mater. Sci. Semicond. Process.* 172 (2024) 108076, <https://doi.org/10.1016/j.mssp.2023.108076>.
- [32] H.R. Chandrasekhar, A.K. Ramdas, S. Rodriguez, Resonant interaction of acceptor states with optical phonons in silicon, *Phys. Rev. B* 14 (1976) 2417, <https://doi.org/10.1103/PhysRevB.14.2417>.
- [33] A. Onton, P. Fisher, A.K. Ramdas, Anomalous width of some photoexcitation lines of impurities in silicon, *Phys. Rev. Lett.* 19 (1967) 780, <https://doi.org/10.1103/PhysRevLett.19.780>.
- [34] F.A. Johnson, Lattice absorption bands in silicon, *Proc. Phys. Soc.* 73 (1959) 265, <https://doi.org/10.1088/0370-1328/73/2/315>.
- [35] D. Franta, D. Nečas, L. Zajíčková, I. Ohlídal, Dispersion model of two-phonon absorption: application to c-Si, *Opt. Mater. Express* 4 (2014) 1641–1656, <https://doi.org/10.1364/OME.4.001641>.
- [36] M. Steger, A. Yang, D. Karaikaj, M.L.W. Thewalt, E.E. Haller, J.W. Ager III, M. Cardona, H. Riemann, N.V. Abrosimov, A.V. Gusev, A.D. Bulanov, A. K. Kaliteevskii, O.N. Godisov, P. Becker, H.-J. Pohl, Shallow impurity absorption spectroscopy in isotopically enriched silicon, *Phys. Rev. B* 79 (2009) 205210, <https://doi.org/10.1103/PhysRevB.79.205210>.
- [37] *Laser Spectroscopy. Vol.2 Experimental Techniques [Demtröder W.]*, fourth ed., Springer, 2008, p. 697p.
- [38] P.T. Greenland, S.A. Lynch, A.F.G. van der Meer, B.N. Murdin, C.R. Pidgeon, B. Redlich, N.Q. Vinh, G. Aeppli, Coherent control of rydberg states in silicon, *Nature* 465 (2010) 1057–1061, <https://doi.org/10.1038/nature09112>.
- [39] S.G. Pavlov, N. Deßmann, A. Pohl, V.B. Shuman, L.M. Portsel, A.N. Lodygin, Yu A. Astrov, S. Winnerl, H. Schneider, N. Stavrias, A.F.G. van der Meer, V. V. Tsyplenkov, K.A. Kovalesky, R. Kh Zhukavin, V.N. Shastin, N.V. Abrosimov, H.-W. Hübers, Dynamics of nonequilibrium electrons on neutral center states of interstitial magnesium donor in silicon, *Phys. Rev. B* 94 (2016) 075208, <https://doi.org/10.1103/PhysRevB.94.075208>.
- [40] N.A. Bekin, R. Kh Zhukavin, V.V. Tsyplenkov, V.N. Shastin, Multi-phonon relaxation of the 1s(T₂) triplet of neutral magnesium donors in silicon, *Semiconductors* 58 (2024) 202–208, <https://doi.org/10.1134/S1063782624030023>.
- [41] N.Q. Vinh, B. Redlich, A.F.G. van der Meer, C.R. Pidgeon, P.T. Greenland, S. A. Lynch, G. Aeppli, B.N. Murdin, Time-resolved dynamics of shallow acceptor transitions in silicon, *Phys. Rev. X* 3 (2013) 011019, <https://doi.org/10.1103/PhysRevX.3.011019>.
- [42] G. Deinzer, D. Strauch, Two-phonon infrared absorption spectra of germanium and silicon calculated from first principles, *Phys. Rev. B* 69 (2004) 045205, <https://doi.org/10.1103/PhysRevB.69.045205>.
- [43] S.G. Pavlov, H.-W. Hübers, P.M. Haas, J.N. Hovenier, T.O. Klaassen, R. Kh Zhukavin, V.N. Shastin, D.A. Carder, B. Redlich, Evidence of noncascade intracenter electron relaxation in shallow donor centers in silicon, *Phys. Rev. B* 78 (2008) 165201, <https://doi.org/10.1103/PhysRevB.78.165201>.